

# Update of the MCSANC Monte Carlo Integrator, v.1.20

A. Arbuzov<sup>b</sup>, D. Bardin<sup>a1</sup>, S. Bondarenko<sup>b</sup>, P. Christova<sup>a</sup>, L. Kalinovskaya<sup>a</sup>,  
U. Klein<sup>d</sup>, V. Kolesnikov<sup>a</sup>, L. Rummyantsev<sup>a,c</sup>, R., Sadykov<sup>a</sup>, A. Sapronov<sup>a</sup>.

<sup>a</sup> Dzhelapov Laboratory of Nuclear Problems, JINR, Joliot-Curie str. 6, 141980  
Dubna, Russia;

<sup>b</sup> Bogoliubov Laboratory of Theoretical Physics, JINR, Joliot-Curie str. 6, 141980  
Dubna, Russia;

<sup>c</sup> Institute of Physics, Southern Federal University, Rostov-on-Don, 344090 Russia;

<sup>d</sup> University of Liverpool, Liverpool, UK.

## Abstract

This article presents new features of the MCSANC v.1.20 program, a Monte Carlo tool for calculation of the next-to-leading order electroweak and QCD corrections to various Standard Model processes. The extensions concern implementation of Drell–Yan-like processes and include a systematic treatment of the photon-induced contribution in proton–proton collisions and electroweak corrections beyond NLO approximation. There are also technical improvements such as calculation of the forward-backward asymmetry for the neutral current Drell–Yan process. The updated code is suitable for studies of the effects due to EW and QCD radiative corrections to Drell–Yan (and several other) processes at the LHC and for forthcoming high energy proton–proton colliders.

## Contents

<b>1</b>	<b>Introduction</b>	<b>1</b>
<b>2</b>	<b>Photon-induced processes</b>	<b>2</b>
<b>3</b>	<b>Leading two-loop electroweak corrections</b>	<b>4</b>
<b>4</b>	<b>Numerical results</b>	<b>6</b>
4.1	Photon-induced processes . . . . .	6
4.2	Higher order corrections . . . . .	6
4.3	Forward-backward asymmetry . . . . .	8
<b>5</b>	<b>Conclusion</b>	<b>8</b>
<b>6</b>	<b>Acknowledgement</b>	<b>9</b>
	<b>References</b>	<b>9</b>

## 1 Introduction

The forthcoming LHC data on Drell–Yan (DY) processes allows to access final states with very high invariant di-lepton masses, where the photon-induced

contributions become substantial relative to the standard quark–antiquark annihilation sub-processes. An accurate estimate of these contributions for hypothetical high mass resonance searches requires the inclusion into the theory predictions sub-processes with photons in the initial  $pp$  state such as  $q\gamma \rightarrow q'\ell^\pm\nu_\ell$ ,  $q\gamma \rightarrow q\ell^+\ell^-$  and  $\gamma\gamma \rightarrow \ell^+\ell^-$ .

Corrections to the neutral current Drell–Yan (NC DY) cross-section due to photon-induced process  $\gamma\gamma \rightarrow \ell^+\ell^-$  can reach up to 10 – 20% for high invariant mass  $M_{\ell^+\ell^-}$  with a choice of kinematic cuts typical for LHC experimental analysis. A first evidence of this kind of background was found by the ATLAS Collaboration in high mass NC DY cross section measurements [1].

Photon-induced Drell–Yan processes were carefully investigated in many papers, see for example [2] and [3].

In the TeV region of invariant masses the higher order two-loop electroweak (EW) and QCD leading terms are important for estimation of the theoretical uncertainties in different EW schemes.

With this paper we continue the series of works [4], [5] dedicated to the development of MCSANC, a Monte Carlo tool based on the SANC modules [6]<sup>2</sup>. We present an update of the integrator up to v.1.20 with inclusion of the aforesaid corrections relevant for DY processes at the LHC at  $\sqrt{s} = 13$  TeV. We briefly review the implementation into the framework of the MCSANC v.1.20 tool the following three new options:

- photon-induced contributions. The implemented processes are:
  - $q\gamma \rightarrow q'\ell^\pm\nu_\ell$  (for CC DY),
  - $q\gamma \rightarrow q\ell^+\ell^-$  (for NC DY),
  - $\gamma\gamma \rightarrow \ell^+\ell^-$  (for NC DY);
- Leading in  $G_\mu m_t^2$  two-loop EW and mixed EW $\otimes$ QCD radiative corrections;
- forward-backward asymmetry  $A_{FB}^{ff}$ .

This paper is organized as follows. In Section 2 we describe the implementation of the photon-induced processes. Section 3 is devoted to the accounting of higher order radiative corrections using the  $\rho$  parameter at two loops. Results of our estimates of photon-induced processes, higher order radiative corrections, and forward-backward asymmetry  $A_{FB}^{ff}$ , as well as comparison between MCSANC v.1.20 and [2] and [7] are presented in Section 4. A brief conclusion is given in Sect. 5.

## 2 Photon-induced processes

The introduction of photon-induced corrections into the SANC environment is presented in paper [3] where the  $\overline{\text{MS}}$  subtraction scheme is realized.

The DIS subtraction scheme can be realized using the sum of the following subtraction terms:

$$\left(\delta_1^{\overline{\text{MS}}} + \delta_1^{\text{DIS}}\right) + \left(\delta_2^{\overline{\text{MS}}} + \delta_2^{\text{DIS}}\right). \quad (1)$$

---

<sup>2</sup>This paper uses the same nomenclature as introduced in [3]

Here  $\delta_1^{\overline{\text{MS}}} = \delta_1(c_1)$ ,  $\delta_2^{\overline{\text{MS}}} = \delta_2(c_1)$  and the corresponding structure function are given by Eqs. (6) and (8) in paper [3]. The structure function

$$D_{q_i \gamma}^{\text{DIS}}(x) = -\log \frac{Q^2(1-x)}{xm_q^2} (x^2 + (1-x)^2) - 1 + 8x - 8x^2 \quad (2)$$

should be used within the kinematics (5) of the above paper. Note that expression (1) is for NC DY processes while only the first two terms in parentheses are present for CC DY ones.

The  $\delta_2^{\text{DIS}}$  contribution is calculated within the following kinematics

$$\begin{aligned} \delta_2^{\text{DIS}} &= \sum_{q_i} \int_{2m_f}^{\sqrt{s_0}} dM \int_{-\infty}^{+\infty} dY \int_0^1 dx_3 \int_{-1}^1 d \cos \hat{\vartheta} q_i(x_1, \mu_F^2) \gamma(x_2, \mu_F^2) \\ &\times \frac{d\hat{\sigma}^{\gamma\gamma}(M, \cos \hat{\vartheta})}{d \cos \hat{\vartheta}} \frac{2M}{x_3 s_0} \Theta(1-x_1) \frac{\alpha}{2\pi} Q_{q_i}^2 \left( C_{\gamma q_i}^{\text{DIS}}(x_3) - \delta(1-x_3) \int_0^1 C_{\gamma q_i}^{\text{DIS}}(z) dz \right) \\ &= \sum_{q_i} \int_{2m_f}^{\sqrt{s_0}} dM \int_{-\infty}^{+\infty} dY \int_0^1 dx_3 \int_{-1}^1 d \cos \hat{\vartheta} \frac{2M}{s_0} \\ &\times \left( \frac{q_i(x_1, \mu_F^2)}{x_3} \Theta(1-x_1) - q_i(\bar{x}_1, \mu_F^2) \Theta(1-\bar{x}_1) \right) \\ &\times \gamma(x_2, \mu_F^2) \frac{d\hat{\sigma}^{\gamma\gamma}(M, \cos \hat{\vartheta})}{d \cos \hat{\vartheta}} D_{\gamma q_i}^{\text{DIS}}(x_3), \end{aligned} \quad (3)$$

where the coefficient function reads

$$C_{\gamma q_i}^{\text{DIS}}(x) = - \left( \frac{1+x^2}{1-x} \left( \log \frac{1-x}{x} - \frac{3}{4} \right) + \frac{9+5x}{4} \right),$$

and

$$\begin{aligned} M &= \sqrt{x_1 x_2 x_3 s_0}, & Y &= \frac{1}{2} \log \frac{x_1 x_3}{x_2}, \\ x_1 &= \frac{M}{\sqrt{s_0}} \frac{e^Y}{x_3}, & \bar{x}_1 &= x_1 x_3, & x_2 &= \frac{M}{\sqrt{s_0}} e^{-Y}, \end{aligned}$$

where  $\sqrt{s_0}$  is the c.m.s. energy of colliding protons. Regularization of function  $C_x$  at  $x \rightarrow 1$  is performed by plus-prescription explicitly shown in (3).

Another sub-process with photons in the initial state is  $\gamma\gamma \rightarrow \ell^+ \ell^-$  which contributes to NC DY only. Here we give only the cross section of the process in the massless case,

$$\hat{\sigma}^{\gamma\gamma, \text{Born}} = \frac{\alpha^2 \pi}{s} \left( \frac{t}{u} + \frac{u}{t} \right), \quad (4)$$

and in the massive case,

$$\begin{aligned} \hat{\sigma}^{\gamma\gamma, \text{Born}} &= \frac{\alpha^2 \pi}{s} \left\{ \frac{1}{1 - \beta_l \cos \vartheta} \left[ 1 + \beta_l \cos \vartheta + \frac{4m_f^2}{s} \left( 1 - \frac{1 + \beta_l^2}{1 - \beta_l \cos \vartheta} \right) \right] \right. \\ &\left. + \frac{1}{1 + \beta_l \cos \vartheta} \left[ 1 - \beta_l \cos \vartheta + \frac{4m_f^2}{s} \left( 1 - \frac{1 + \beta_l^2}{1 + \beta_l \cos \vartheta} \right) \right] \right\}, \end{aligned} \quad (5)$$

where  $\beta_l = \beta(s, m_l^2, m_l^2) = \sqrt{1 - 4 \frac{m_l^2}{s}}$  and  $\vartheta$  is the angle between the photon and outgoing lepton momenta in the center-of-mass system.

### 3 Leading two-loop electroweak corrections

In MCSANC v.1.20 we follow the recipe introduced in Refs. [8] and [9], and later well described in Ref [10].

The  $\rho$  parameter is defined as the ratio of the neutral current to charged current amplitudes at zero momentum transfer, see for example [8]:

$$\rho = \frac{G_{NC}(0)}{G_{CC}(0)} = \frac{1}{1 - \Delta\rho}, \quad (6)$$

where  $G_{CC}(0) = G_\mu$  is the Fermi constant defined from the  $\mu$ -decay width, and the quantity  $\Delta\rho$  is treated perturbatively

$$\Delta\rho = \Delta\rho^{(1)} + \Delta\rho^{(2)} + \dots \quad (7)$$

Expanding (6) up to quadratic terms  $\Delta\rho^2$ , we have

$$\rho = 1 + \Delta\rho + \Delta\rho^2. \quad (8)$$

The contribution to  $\Delta\rho$ , leading in  $G_\mu m_t^2$  NLO EW, is explicitly given by

$$\Delta\rho^{(1)} \Big|^{G_\mu} = 3x_t = \frac{3\sqrt{2}G_\mu m_t^2}{16\pi^2}. \quad (9)$$

At the two-loop level, the quantity  $\Delta\rho$  contains two contributions:

$$\Delta\rho = N_c x_t \left[ 1 + \rho^{(2)} \left( m_H^2/m_t^2 \right) x_t \right] \left[ 1 - \frac{2\alpha_s(m_Z^2)}{9\pi} (\pi^2 + 3) \right]. \quad (10)$$

They consist of the following:

i) two-loop EW part at  $\mathcal{O}(G_\mu^2)$ , second term in the first square brackets [11], [8] and [9] with  $\rho^{(2)}$  given in Eq. (12) of [9] (actually, after discovery of the Higgs boson and determination of its mass, it has become sufficient to use the low Higgs mass asymptotic, Eq. (15), of [9]);

ii) mixed two-loop EW $\otimes$ QCD at  $\mathcal{O}(G_\mu\alpha_s)$ , the second term in the second square brackets, see in [12]–[13] for further details.

From Eq. (6), using intermediate vector boson propagators  $\sim 1/(Q^2 + M_V^2)$ , we derive:

$$\rho = \frac{m_W^2}{\bar{c}_W^2 m_Z^2}, \quad (11)$$

where we have introduced a new parameter  $\bar{c}_W^2$  to distinguish from the usual  $c_W^2$  for which we maintain the meaning  $c_W^2 = m_W^2/m_Z^2$  to be valid to all perturbative orders. At the lowest order (LO)

$$\rho^{(0)} = \frac{m_W^2}{c_W^2 m_Z^2} = 1. \quad (12)$$

From Eq.(11) we have:

$$\bar{c}_W^2 = \frac{m_W^2}{\rho m_Z^2} = (1 - \Delta\rho) c_W^2. \quad (13)$$

The universal higher order (h.o.) corrections, leading in  $G_\mu m_t^2$ , may be taken into account via the following replacements:

$$\alpha_{G_\mu} \rightarrow \alpha_{G_\mu} \frac{\bar{s}_W^2}{s_W^2}, \quad (14)$$

$$s_W^2 \rightarrow \bar{s}_W^2 \equiv s_W^2 + \Delta\rho c_W^2, \quad c_W^2 \rightarrow \bar{c}_W^2 \equiv 1 - \bar{s}_W^2 = (1 - \Delta\rho) c_W^2 \quad (15)$$

in the LO expression for NC DY cross section (see discussion after Eq.(3.48)) of [7]).

As was argued in Refs. [14], [15] and [8], this approach correctly reproduces terms up to  $\mathcal{O}(\Delta\rho^2)$ .

Given the replacements in Eq.(15), we get the following contributions of h.o. EW corrections to the scalar form factors<sup>3</sup> of the invariant amplitude. In the  $G_\mu$ -scheme,

$$\alpha_{G_\mu} = \frac{\sqrt{2}G_\mu m_W^2 s_W^2}{\pi}, \quad (16)$$

the form factor  $\mathcal{F}_\gamma$  of  $\gamma$  exchange effectively contains the factor  $s_W^2$

$$\alpha_{G_\mu} \mathcal{F}_\gamma \rightarrow \alpha_{G_\mu} \bar{s}_W^2 / s_W^2 = \alpha_{G_\mu} \left( 1 + \frac{c_W^2}{s_W^2} \Delta\rho \right), \quad (17)$$

while four form factors of  $Z$  exchange,  $\mathcal{F}_Z^{LL}$ ,  $\mathcal{F}_Z^{LQ}$ ,  $\mathcal{F}_Z^{QL}$ ,  $\mathcal{F}_Z^{QQ}$ , contain a common factor  $1/c_W^2$ . We consider  $\mathcal{F}_Z^{LL}$  as an example

$$\alpha_{G_\mu} \kappa \mathcal{F}_Z^{LL} = \alpha_{G_\mu} \frac{1}{4s_W^2 c_W^2} \mathcal{F}_Z^{LL}. \quad (18)$$

Since the coupling factor  $\alpha_{G_\mu}/s_W^2$  does not receive universal corrections, as follows from Eq.(17), we should insert only factors which come from  $1/c_W^2$ ,

$$\alpha_{G_\mu} \frac{1}{4s_W^2 c_W^2} \mathcal{F}_Z^{LL} \rightarrow \alpha_{G_\mu} \frac{1}{4s_W^2 \bar{c}_W^2} = \alpha_{G_\mu} \frac{1}{4s_W^2 c_W^2} (1 + \Delta\rho + \Delta\rho^2). \quad (19)$$

In addition to Eq.(19), form factors  $\mathcal{F}_Z^{LQ,QL}$  of  $Z$  exchange contain the factor  $s_W^2$  and form factor  $\mathcal{F}_Z^{QQ}$  contains the factor  $s_W^4$ . Therefore, form factors at NNLO order read:

$$\begin{aligned} \mathcal{F}_\gamma^{QQ} &= 1 + \frac{c_W^2}{s_W^2} \Delta\rho, \\ \mathcal{F}_Z^{LL} &= 1 + \Delta\rho + \Delta\rho^2, \\ \mathcal{F}_Z^{LQ} &= (1 + \Delta\rho + \Delta\rho^2) \left( 1 + \frac{c_W^2}{s_W^2} \Delta\rho \right), \\ \mathcal{F}_Z^{QL} &= (1 + \Delta\rho + \Delta\rho^2) \left( 1 + \frac{c_W^2}{s_W^2} \Delta\rho \right), \\ \mathcal{F}_Z^{QQ} &= (1 + \Delta\rho + \Delta\rho^2) \left( 1 + \frac{c_W^2}{s_W^2} \Delta\rho \right)^2. \end{aligned} \quad (20)$$

To avoid double counting one should remove the leading NLO EW contribution (9) from the terms linear in  $\Delta\rho$ :  $\Delta\rho \rightarrow \left( \Delta\rho - \Delta\rho^{(1)} \Big|^{G_\mu} \right)$ .

Eqs.(20) were realized in new `modules` which compute the differential cross section contributions taking into account terms up to the order  $\mathcal{O}(\Delta\rho)$  (`ih0=1`) or  $\mathcal{O}(\Delta\rho^2)$  (`ih0=2`).

We have shown analytically that the results obtained in this way agree with the corresponding expressions derived in [7].

---

<sup>3</sup>For the definition of the scalar form factors see Eqs.(29)–(30) in [16].

## 4 Numerical results

### 4.1 Photon-induced processes

In Tables 1 and 2 we present the LO inclusive cross sections for the process  $pp \rightarrow e^+ \nu_e X$  and the photon-induced contributions  $\delta_{q/\bar{q}\gamma} = \frac{\sigma_{q/\bar{q}\gamma}}{\sigma_0}$  for different ranges of the lepton pair transverse mass  $M_{T,l\nu}$  and of the transverse momentum  $p_{T,l}$ , respectively. For the sake of comparison we used the setup and input parameters from the paper [2]. Results of MCSANC (first line) are compared to the ones presented in Table 1 of [2] (second line). The lowest order cross sections are given in picobarns, the correction factors are shown in %. The numbers illustrate good agreement within the statistical errors of Monte Carlo integration.

$M_{T,l\nu}/\text{GeV}$	$\sigma_0/\text{pb}$	$\delta_{q/\bar{q}\gamma}/\%$
50- $\infty$	4495.8(1)	0.047(3)
	4495.7(2)	0.052(1)
100- $\infty$	27.590(1)	0.11(1)
	27.589(2)	0.12(1)
200- $\infty$	1.7907(1)	0.24(1)
	1.7906(1)	0.25(1)
500- $\infty$	0.084696(1)	0.36(1)
	0.084697(4)	0.37(1)
1000- $\infty$	0.0065221(1)	0.38(1)
	0.0065222(4)	0.39(1)
2000- $\infty$	0.00027322(1)	0.35(1)
	0.00027322(1)	0.36(1)

Table 1: Comparison of the LO and  $\delta_{q/\bar{q}\gamma}$  for  $pp \rightarrow e^+ \nu_e X$  in  $M_{T,l\nu}$  bins between MCSANC and [2].

In the same setup, in Tables 3 and 4 we present the LO inclusive cross sections for processes  $pp \rightarrow e^- \nu_e X$  and the photon-induced contributions  $\delta_{q/\bar{q}\gamma}$ .

In Table 5 we present the LO cross section for the process  $pp \rightarrow e^+ e^- X$ ,  $\sigma_0$  in pb, and the corresponding contributions of photon-induced process  $\delta_{q/\bar{q}\gamma}$  (column 3) and  $\delta_{\gamma\gamma} = \frac{\sigma_{\gamma\gamma,0}}{\sigma_0}$  (column 4). Here we used the setup and input parameters given in [7]. The results of the MCSANC integrator are in the first rows, and the ones from Ref. [7] are in the second rows. Excellent agreement between these two calculations is observed.

In the programs' user interface these corrections are controlled by a new `iph` flag added to the `ifl` parameter list. Setting `iph=0` disables photon-induced contributions, `iph=1` includes the  $q\gamma \rightarrow q\ell^+\ell^-$  (NC DY) and  $q\gamma \rightarrow q'\ell^\pm\nu$  (CC DY) components, and `iph=2` includes the  $\gamma\gamma \rightarrow \ell^+\ell^-$  (NC DY) contributions.

### 4.2 Higher order corrections

In Table 5 we present the inclusive LO cross section  $\sigma_0$  in pb for the process  $pp \rightarrow e^+ e^- X$  and the corresponding higher order corrections  $\delta_{h.o.weak} =$

$p_{T,l}/\text{GeV}$	$\sigma_0/\text{pb}$	$\delta_{q/\bar{q}\gamma}/\%$
25- $\infty$	4495.8(1)	0.059(3)
	4495.7(2)	0.065(1)
50- $\infty$	27.590(1)	4.6(1)
	27.589(2)	4.7(1)
100- $\infty$	1.7907(1)	11.9(1)
	1.7906(1)	12.3(1)
200- $\infty$	0.18129(1)	16.6(1)
	0.18128(1)	17.1(1)
500- $\infty$	0.0065221(1)	16.2(1)
	0.0065222(4)	16.7(1)
1000- $\infty$	0.00027322(1)	13.1(1)
	0.00027322(1)	13.5(1)

Table 2: Comparison of the LO cross section and  $\delta_{q/\bar{q}\gamma}$  for  $pp \rightarrow e^+\nu_e X$  in  $p_{T,l}$  bins between MCSANC and [2].

$M_{T,l-\nu}/\text{GeV}$	$\sigma_0/\text{pb}$	$\delta_{q/\bar{q}\gamma}/\%$
50- $\infty$	3436.2(1)	0.068(2)
100- $\infty$	20.037(1)	0.113(4)
200- $\infty$	1.08169(1)	0.223(2)
500- $\infty$	0.042127(1)	0.328(3)
1000- $\infty$	0.002584(1)	0.349(3)
2000- $\infty$	0.00008049(1)	0.344(3)

Table 3: The LO results and  $\delta_{q/\bar{q}\gamma}$  for  $pp \rightarrow e^-\nu_e X$  in  $M_{T,l\nu}$  bins.

$p_{T,l-}/\text{GeV}$	$\sigma_0/\text{pb}$	$\delta_{q/\bar{q}\gamma}/\%$
25- $\infty$	3436.2(1)	0.060(2)
50- $\infty$	20.037(1)	5.30(1)
100- $\infty$	1.0812(1)	16.22(2)
200- $\infty$	0.09503(1)	26.31(2)
500- $\infty$	0.002584(1)	34.87(4)
1000- $\infty$	0.00008049(1)	39.72(2)

Table 4: The LO results and  $\delta_{q/\bar{q}\gamma}$  for  $pp \rightarrow e^-\nu_e X$  in  $p_{T,l}$  bins.

$\frac{\sigma_{h.o.weak}}{\sigma_0}$  (column 5). The setup and the input parameters are taken from paper [7]. The first rows represent results of the MCSANC integrator and the second ones show the numbers computed in [7]. Again we see excellent agreement between these two calculations.

In the programs' user interface the higher order corrections are controlled by a new `ih0` flag added to the `iflew` parameter list. Setting `ih0=0` disables higher order correction contributions, `ih0=1` includes linear  $\left(\Delta\rho - \Delta\rho^{(1)}\right)^{G_\mu}$

$M_{ll}/\text{GeV}$	$\sigma_0/\text{pb}$	$\delta_{q/\bar{q}\gamma}/\%$	$\delta_{\gamma\gamma,0}/\%$	$\delta_{h.o.weak}/\%$
50- $\infty$	738.813(5)	-0.105(1)	0.17(1)	0.030(1)
	738.773(6)	-0.11	0.17	0.030
100- $\infty$	32.7293(2)	-0.207(1)	1.16(1)	0.013(1)
	32.7268(3)	-0.21	1.15	0.012
200- $\infty$	1.48488(1)	0.381(1)	4.30(1)	-0.23(1)
	1.48492(1)	0.38	4.30	-0.23
500- $\infty$	0.080942(3)	1.522(1)	4.92(1)	-0.29(1)
	0.0809489(6)	1.53	4.92	-0.29
1000- $\infty$	0.0067998(1)	1.901(1)	5.21(1)	-0.31(1)
	0.00680008(3)	1.91	5.21	-0.31
2000- $\infty$	0.00030375(1)	2.343(1)	6.18(1)	-0.31(1)
	0.000303767(1)	2.34	6.17	-0.32

Table 5: The LO cross section  $\sigma_0$  of  $pp \rightarrow e^+e^-X$  in pb, the contributions of  $(q\gamma)$  and  $(\gamma\gamma)$  configurations in the initial  $pp$  state:  $\delta_{q/\bar{q}\gamma}$  and  $\delta_{\gamma\gamma,0}$ , and higher order corrections  $\delta_{h.o.weak}$  (`ih=2`). Results of MCSANC (first rows) are compared to numbers from Ref.[7] (second rows).

term contributions while `ih=2` includes both linear and quadratic  $\Delta\rho^2$  term contributions.

### 4.3 Forward-backward asymmetry

The forward-backward asymmetry  $A_{FB}^{ff}$  is usually defined as (see [17]):

$$A_{FB} = \frac{F - B}{F + B} \quad (21)$$

where

$$F = \int_0^1 \frac{d\sigma}{d\cos\vartheta^*} d\cos\vartheta^*, \quad B = \int_{-1}^0 \frac{d\sigma}{d\cos\vartheta^*} d\cos\vartheta^*. \quad (22)$$

The cosine of the angle between the lepton and quark in the  $\ell^+\ell^-$  rest frame is then approximated by

$$\begin{aligned} \cos\vartheta^* &= \frac{|p_z(l^+l^-)|}{p_z(l^+l^-)} \cdot \frac{2}{m(l^+l^-)\sqrt{m^2(l^+l^-) + p_T^2(l^+l^-)}} \\ &\times [p^+(l^-)p^-(l^+) - p^-(l^-)p^+(l^+)] \end{aligned} \quad (23)$$

where  $E$  is the energy,  $p_z$  and  $p_T$  are the longitudinal and transverse components of the momentum vector, respectively, and  $p^\pm = \frac{1}{\sqrt{2}}(E \pm p_z)$ .

The MCSANC results for the forward-backward asymmetries (Figure 1) were compared with the ones from Ref. [17]. A good agreement was found.

## 5 Conclusion

In this paper we have presented an update of the MCSANC integrator up to v.1.20. The new features include systematic treatment of the photon-induced



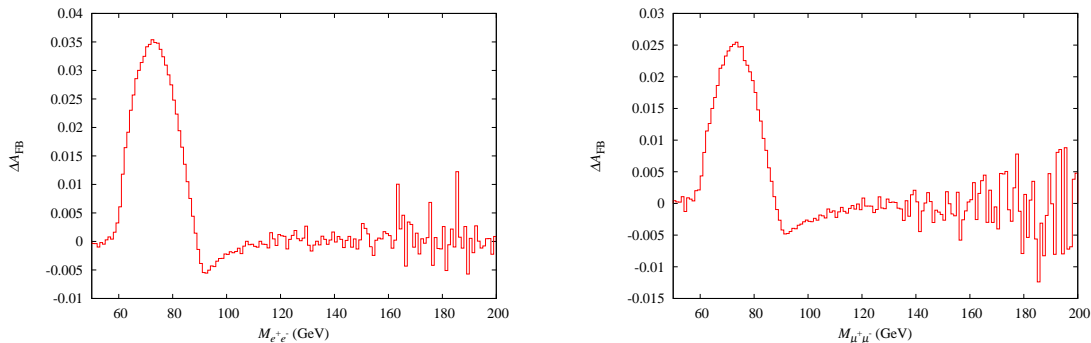


Figure 1: The forward-backward asymmetry  $A_{FB}^{ff}$  of  $pp \rightarrow \ell^+ \ell^- X$  processes for the  $e^+e^-$  (left) and  $\mu^+\mu^-$  (right) cases with bare event selection setups.

contribution in proton–proton collisions and electroweak corrections beyond NLO approximation. The results of the calculations were compared with the results of other theoretical groups showing excellent agreement. The current version of MCSANC v.1.20 is adjusted for studies of various effects due to EW and QCD radiative corrections to realistic LHC observables.

## 6 Acknowledgement

We are grateful to W. von Schlippe for a critical reading of this text and useful comments. The work of L. Rummyantsev was supported by the Institute of Physics theme N 213.01-2014/013-VG ”Analysis of data and modelling states of the near space and the deep space for the purposes of communications and navigation”.

## References

- [1] ATLAS Collaboration, G. Aad *et al.*, *Phys.Lett.* **B725** (2013) 223–242, 1305.4192.
- [2] S. Breusung, S. Dittmaier, M. Kramer, and A. Muck, *Phys.Rev.* **D77** (2008) 073006, 0710.3309.
- [3] A. Arbuzov and R. Sadykov, *J.Exp.Theor.Phys.* **106** (2008) 488–494, 0707.0423.
- [4] D. Bardin, S. Bondarenko, P. Christova, L. Kalinovskaya, L. Rummyantsev, *et al.*, *JETP Lett.* **96** (2012) 285–289, 1207.4400.
- [5] S. G. Bondarenko and A. A. Saprionov, *Comput.Phys.Commun.* **184** (2013) 2343–2350, 1301.3687.
- [6] A. Andonov, A. Arbuzov, D. Bardin, S. Bondarenko, P. Christova, *et al.*, *Comput.Phys.Commun.* **181** (2010) 305–312, arXiv:0812.4207.
- [7] S. Dittmaier and M. Huber, *JHEP* **1001** (2010) 060, 0911.2329.
- [8] J. Fleischer, O. Tarasov, and F. Jegerlehner, *Phys.Lett.* **B319** (1993) 249–256.

- [9] J. Fleischer, O. Tarasov, and F. Jegerlehner, *Phys.Rev.* **D51** (1995) 3820–3837.
- [10] D. Y. Bardin, W. Hollik, and G. Passarino, *Reports of the Working Group on precision calculations for the Z resonance*. CERN 95-03, Geneva, 1995.
- [11] R. Barbieri, M. Beccaria, P. Ciafaloni, G. Curci, and A. Vicere, *Phys.Lett.* **B288** (1992) 95–98, [hep-ph/9205238](#).
- [12] A. Djouadi and C. Verzegnassi, *Phys.Lett.* **B195** (1987) 265.
- [13] A. Djouadi, *Nuovo Cim.* **A100** (1988) 357.
- [14] M. Consoli, W. Hollik, and F. Jegerlehner, *Phys.Lett.* **B227** (1989) 167.
- [15] M. Consoli, W. Hollik, and F. Jegerlehner, *Electroweak Radiative Corrections for Z Physics*, vol. 51. CERN-TH-5527-89, Geneva, 1989.
- [16] A. Andonov, A. Arbuzov, D. Bardin, S. Bondarenko, P. Christova, *et al.*, *Comput.Phys.Commun.* **174** (2006) 481–517, [hep-ph/0411186](#).
- [17] C. Buttar, J. D’Hondt, M. Kramer, G. Salam, M. Wobisch, *et al.*, [arXiv:0803.0678](#).